

Description of TEAM Workshop Problem 29: Whole body cavity resonator

Yasushi Kanai

Department of Information and Electronics Engineering, Niigata Institute of Technology, Kashiwazaki 945-1195, JAPAN
Tel: +81-257-22-8127, fax +81-257-22-8122, E-mail: kanai@iee.niit.ac.jp.

I. INTRODUCTION

TEAM Workshop problem 29, whole body cavity resonator, is described. We have called this resonator a reentrant resonant cavity applicator [1, 2]. The cavity was originally invented for a hyperthermic cancer therapy. Inside the resonator a disk-shaped lossy dielectric phantom is placed, then the radio frequency electromagnetic energy is supplied. Because the resonant state should be kept during the heating process, it is important to derive accurate resonant frequencies before the experiment. Two types of models shall be considered: 1) a disk-shaped lossy dielectric phantom is considered and 2) no phantom is inside the cavity resonator. A steady state high frequency problem shall be solved to obtain the resonant frequencies. Then the calculated values are compared with the measured ones.

II. DESCRIPTION OF THE MODEL

Figures 1-4 show the block diagram of the hyperthermic system, the arrangement of two reentrants, the feeding and sensing coils, the circuit of the feeding coil and the variable capacitor, the shape of the feeding coil, respectively. The electromagnetic energy is supplied through the feeding coil and the field distribution is observed by the sensing coil, where the sensing coil has a diameter of 60 mm. Figure 5 shows the model to be solved as TEAM Workshop problem 29. Note here that the feeding and sensing coils are not shown in the same figure.

The cavity has a diameter of 1900 mm and a height of 1450 mm, therefore, it has enough space to accommodate one adult. Inside the cavity there are two reentrants so that the electromagnetic energy can be concentrated between them. Because we want to apply the electromagnetic energy at the lowest resonant frequency, obtaining the resonant frequencies by calculation is very important. Two types of problems shall be solved: one has a phantom inside the cavity and the other has no phantom inside.

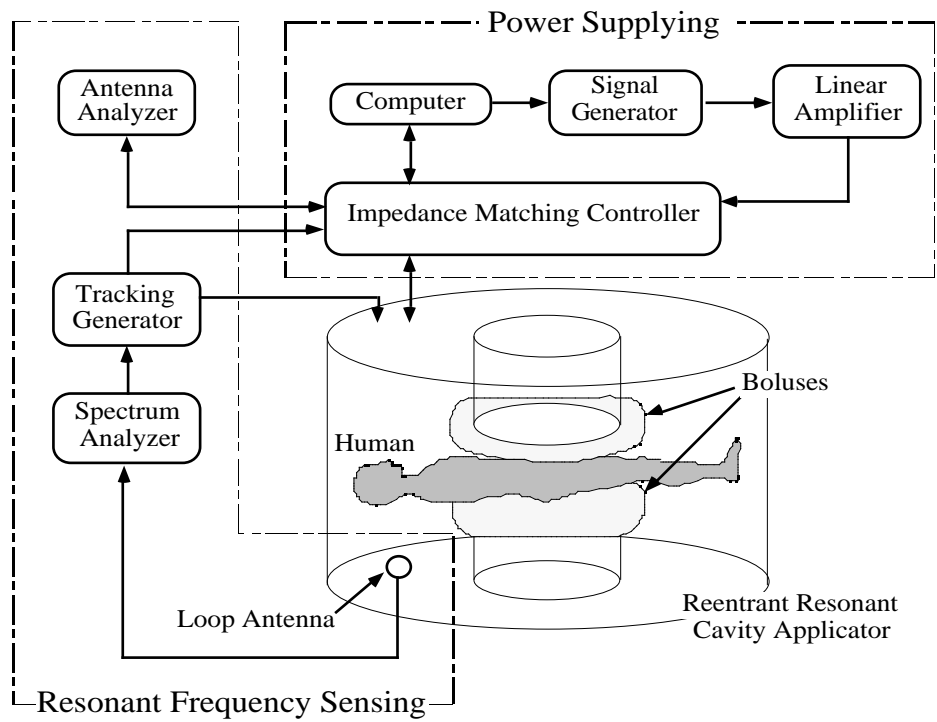


Fig. 1. Blockdiagram of the hyperthermic system.

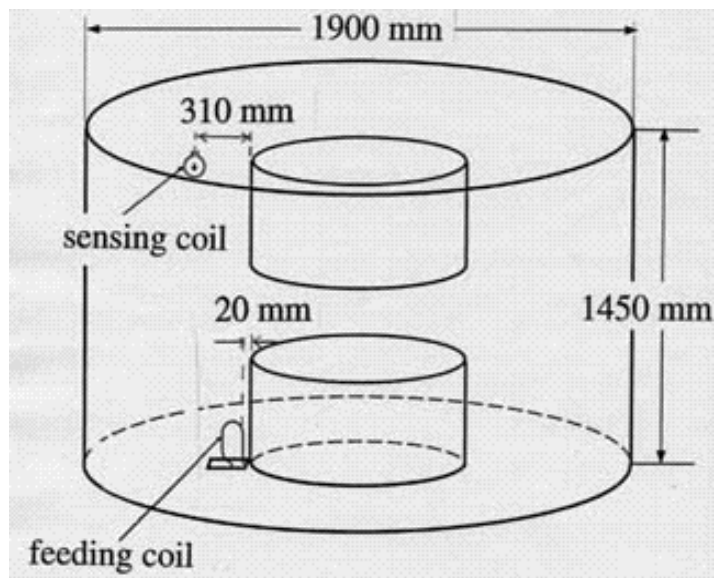


Fig. 2. Arrangement of two reentrants, feeding and sensing coils.

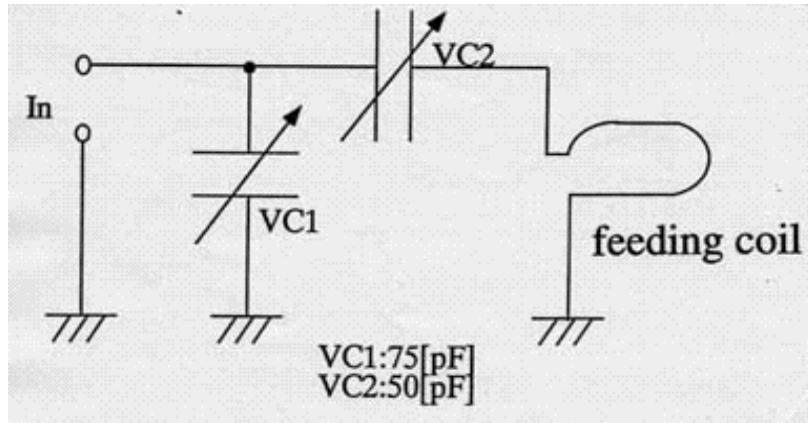


Fig. 3. Electrical circuits of feeding coil and variable capacitors.

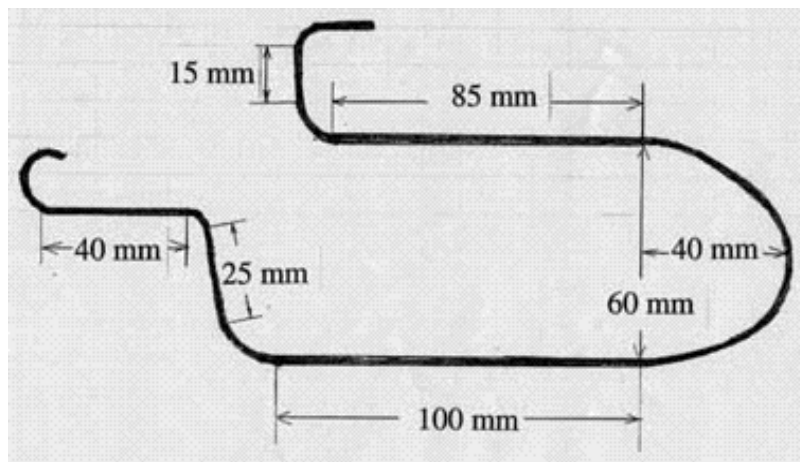


Fig. 4. Shape of the feeding coil.

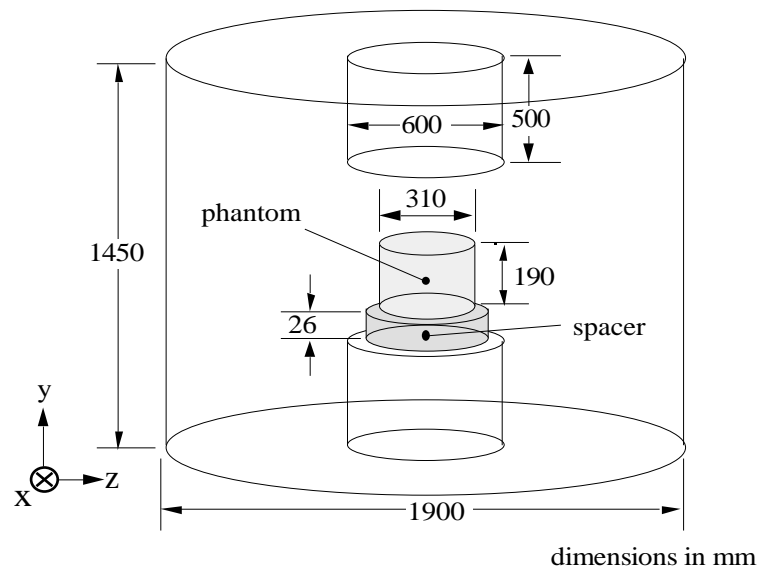


Fig. 5 TEAM Workshop problem 29 to be solved, where feeding and sensing coils are not shown.

As shown in Fig. 6 the electrical constants of the dielectric phantom are strongly dependent on the temperature. Therefore, two cases should be calculated when the dielectric phantom is considered:

a) $\epsilon_r = 80$ and $\sigma = 0.52$, which corresponds to the phantom temperature of 10 °C and

b) $\epsilon_r = 74$ and $\sigma = 0.78$, which corresponds to the phantom temperature of 30 °C.

Namely, three models shall be considered. Note here that the shape of the coil does not affect the resonant frequencies very much, therefore, the shape can be simplified.

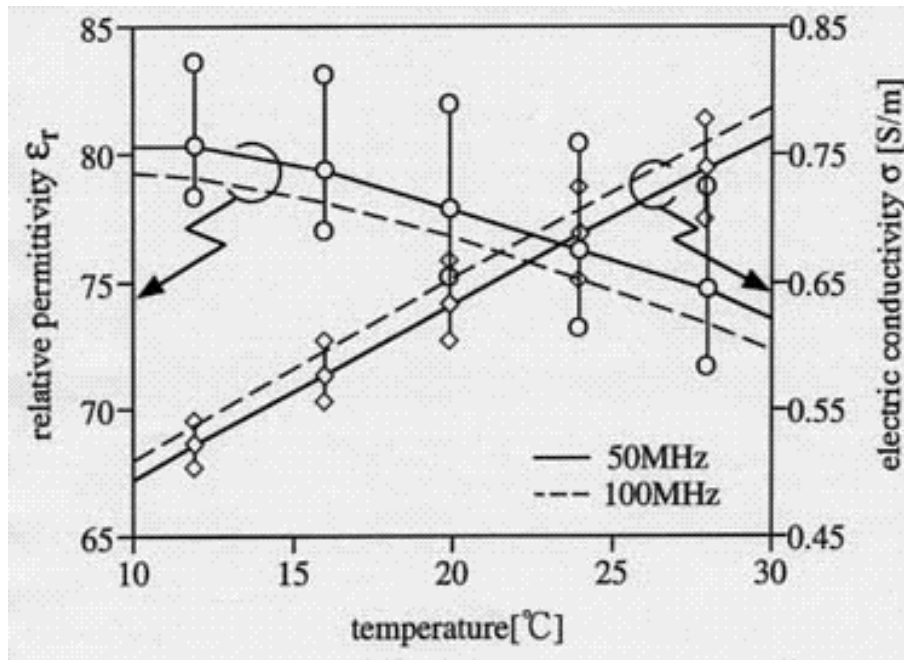


Fig. 6. Temperature dependences of electrical constants.

III. MEASUREMENT OF THE FREQUENCY RESPONSES FOR THE CAVITY

Figures 7 and 8 show the magnetic field measured by the sensing coil with and without the dielectric phantom, respectively. As can be seen from the figures, the first, second and third lowest resonant frequencies are clear, on the other hand, the fourth and higher resonant modes are vague for both cases. Therefore, the first, second and third lowest frequencies should be derived as TEAM problem 29. There were no temperature data of the dielectric phantom when the measurements were performed. The relationship between the resonant frequencies and the temperature of the dielectric phantom will be discussed in IV.

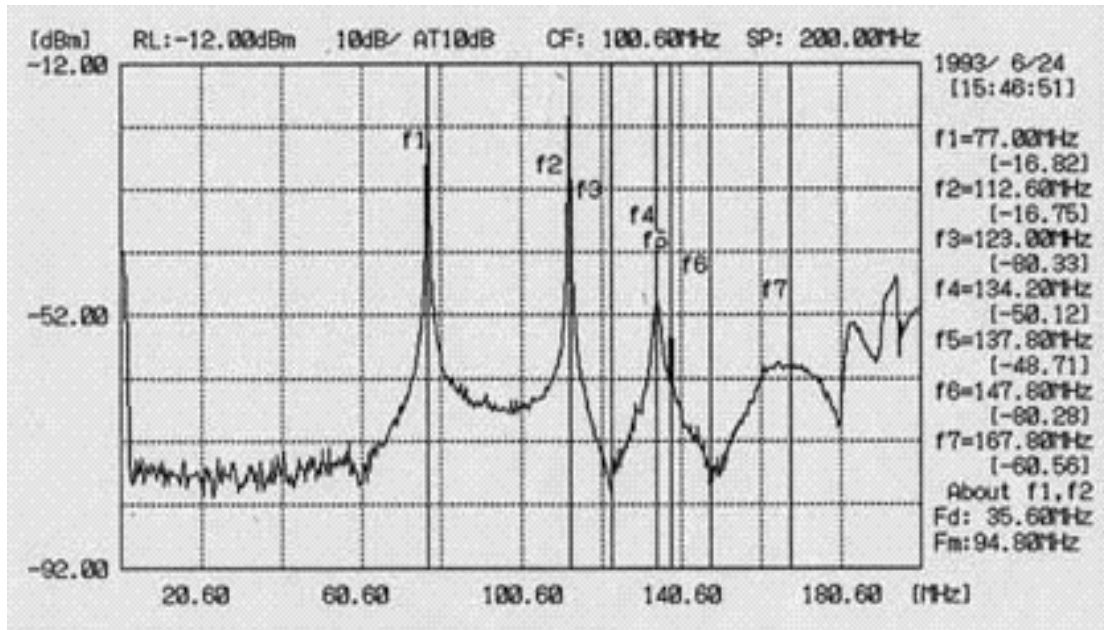


Fig. 7. Measured Results without dielectric phantom inside.

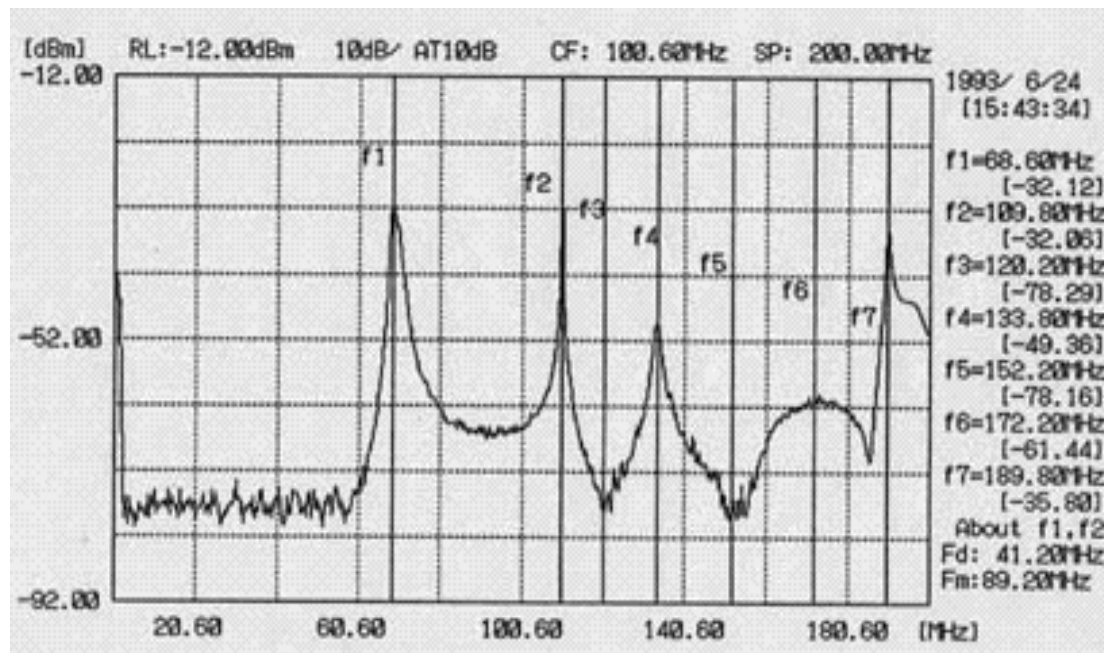


Fig. 8. Measured Results with dielectric phantom (310 mm diameter and 190 mm height) between two reentrants.

IV. CALCULATED RESULTS

We have used the three-dimensional Finite Difference Time Domain (FD-TD) method to solve Maxwell's equations:

$$\nabla \times \mathbf{E} = -\mu \frac{\mathbf{H}}{t}, \quad \nabla \times \mathbf{H} = \mathbf{E} + \frac{\mathbf{E}}{t} \quad (1)$$

Gaussian pulse is added at the location of feeding coil and the field is observed at the point of the observing coil. Resonant frequencies are obtained by the frequency responses as shown in Fig. 9.

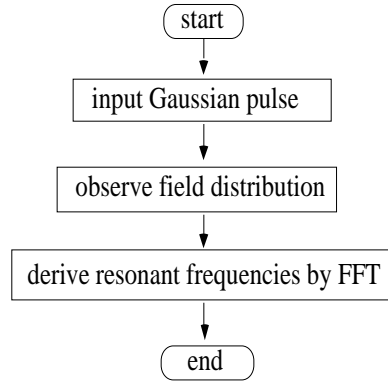


Fig. 9. Flow diagram of the FD-TD calculations.

The model is divided into 41,876 (= 38 x 29 x 38) regular cells with a side length of 50 mm by our automatic mesh generator [3]. We have also calculated using a fine mesh with a side length of 25 mm, which has 335,008 (=76 x 58 x 76) regular cells. Note here that the dimensions of the calculation models are slightly different (phantom diameter 300 mm, height 200 mm, spacer thickness 25 mm or 50 mm) from the experimental one (phantom diameter 310 mm, height 190 mm, spacer thickness 26 mm) because we have used the regular cell models.

Table I shows the comparisons of resonant frequencies when the phantom is not considered. Table II shows the comparisons of resonant frequencies when the phantom is considered. Note here that there were no differences of resonant frequencies for two cases (a) $r = 80$ and $\epsilon = 0.52$, b) $r = 74$ and $\epsilon = 0.78$.

From these two tables, a good agreement can be found for the second and third lowest resonant frequencies while there is a small difference between the values obtained for the lowest resonant frequency. We have already found that the lowest resonant frequency is dependent upon the object between the two reentrants, while the second and third lowest resonant frequencies are from the cavity itself [3]. A finer mesh is required in order to obtain a more accurate value for the lowest resonant frequency.

Interestingly, the third lowest resonant frequency can not be found when 50 mm mesh model is used in spite of that the wave length is fairly larger than the cell size (50mm) even in the dielectric phantom.

TABLE I
COMPARISONS OF RESONANT FREQUENCIES IN MHz,
WHERE PHANTOM IS NOT CONSIDERED

resonance mode	measured	FD-TD 50 mm mesh	FD-TD 25 mm mesh
1st	77	71.9	71.8
2nd	113	110	108
3rd	134	N/A	136

TABLE II
COMPARISONS OF RESONANT FREQUENCIES IN MHz,
WHERE PHANTOM IS CONSIDERED

resonance mode	measured	FD-TD 50 mm mesh	FD-TD 25 mm mesh
1st	68.6	66.3	67
2nd	110	110	110
3rd	134	N/A	134

IV. SUMMARY

TEAM Workshop problem 29, a whole body cavity resonator, has been described. The measured resonant frequencies are shown for two cases: 1) a disk-shaped lossy dielectric phantom is considered and 2) no phantom is inside the cavity resonator. Also, comparisons between the measured and calculated resonant frequencies for two cases have been made.

REFERENCES

- [1] Y. Kanai, T. Tsukamoto, K. Toyama, Y. Saitoh, M. Miyakawa and T. Kashiwa, "Analysis of a hyperthermic treatment in a reentrant resonant cavity applicator by solving time-dependent electromagnetic-heat transfer equations," *IEEE Trans. Magn.*, vol. 32, pp.1661-1664, May 1996.
- [2] Y. Kanai, T. Tsukamoto, Y. Saitoh, M. Miyakawa and T. Kashiwa, "Analysis of a hyperthermic treatment using a reentrant resonant cavity applicator for a heterogeneous model with blood flow," *IEEE Trans. on Magn.*, vol. 33, No. 2, pp. 2175-2178, Mar. 1997.
- [3] Y. Kanai and K. Sato, "Automatic mesh generation for 3D electromagnetic field analysis by FD-TD method," *IEEE Trans. on Magn.*, vol. 34, No.5, Sep. 1998 (in press).